

The Impact of Diethyl Furan-2,5-dicarboxylate as an Aromatic Biobased Monomer toward Lipase-Catalyzed Synthesis of Semiaromatic Copolyesters

Kifah Nasr, Audrey Favrelle-Huret, Rosica Mincheva, Gregory Stoclet, Marc Bria, Jean-Marie Raquez,* and Philippe Zinck*



Cite This: <https://doi.org/10.1021/acscapm.1c01777>



Read Online

ACCESS |



Metrics & More



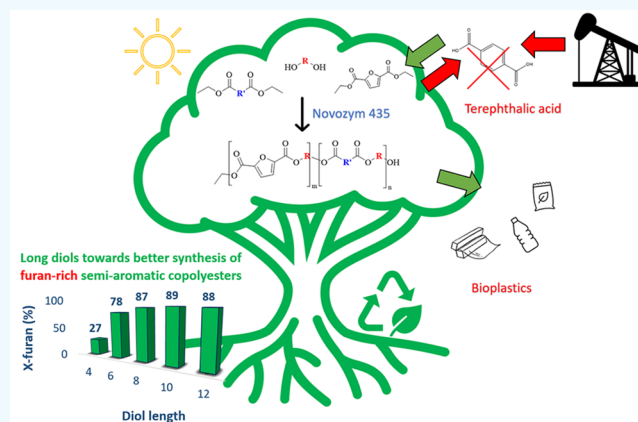
Article Recommendations



Supporting Information

ABSTRACT: Furan-2,5-dicarboxylic acid has been introduced in recent years as a green aromatic monomer toward the design of aromatic (co)polyesters with enhanced properties, i.e., polyethylene furanoate (PEF) that can definitely compete with its petroleum-based counterpart, i.e., polyethylene terephthalate (PET). In an attempt to produce biobased semiaromatic copolyesters in an efficient eco-friendly approach, we report herein the polycondensation of diethyl furan-2,5-dicarboxylate (DEFDC) with different aliphatic diols and diesters of variable chain length catalyzed by an immobilized lipase from *Candida antarctica* using a two-step polymerization reaction carried out in diphenyl ether. The influence of diol and diester chain length, the molar concentration of DEFDC, and the effect of enzyme loading were assessed via nuclear magnetic resonance (NMR), gel permeation chromatography (GPC), differential scanning calorimetry (DSC), and wide-angle X-ray scattering (WAXS). With high quantities of DEFDC, significant differences in terms of \bar{M}_n buildup were noticed. Only longer diols starting from octane-1,8-diol successfully reacted with up to 90% DEFDC as opposed to only 25% DEFDC reacting with short diols such as butane-1,4-diol. While varying the chain length of the diester, it was evident that shorter diols such as hexane-1,6-diol have better reactivity toward longer diesters, while dodecane-1,12-diol was reactive toward all tested diesters. The incorporation of long chain fatty dimer diols such as Pripol 2033 led to polyesters with higher \bar{M}_n and was successfully used to overcome the limitations of poor reactivity observed in the case of short diols in the presence of high furan content. The DSC results showed a pseudoeutectic behavior as a function of increasing the mol % of DEFDC, and a change in the crystalline phase was confirmed via WAXS analysis. Finally, this work showed the successful enzyme-catalyzed synthesis of several DEFDC biobased semiaromatic copolyesters with variable interesting properties that can be further optimized for possible applications in food packaging as well as other possibilities.

KEYWORDS: enzymatic polymerization, polycondensation, lipase, furan, aromatic copolyesters, time course profile



INTRODUCTION

The increasing environmental concerns of fossil fuel-based materials and their pronounced negative impact on our environment has been shifting the research focus toward a more sustainable synthetic pathway to develop polymers with adequate properties and a low carbon footprint. Such an approach is strongly supported with the increasing research works on the valorization of biomass to produce biobased polymeric materials.^{1–5} In this respect, furan-2,5-dicarboxylic acid (FDCA) has been given a lot of attention in recent years as a (co)monomer, due to its ease of production from biomass and its aromaticity. FDCA is a biobased monomer synthesized by oxidation of 5-hydroxymethylfurfural, which is by turn the dehydration product of hexoses such as fructose and

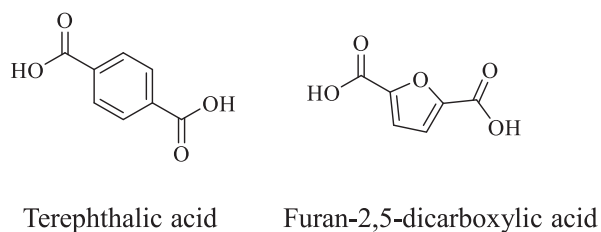
glucose.^{6–8} There are many new research works that implement FDCA as an alternative (co)monomer to petroleum-based terephthalic acid (TPA), which is vastly used in the synthesis of aromatic polyesters, notably polyethylene terephthalate (PET) and polybutylene terephthalate (PBT). This trend favoring FDCA stems from the structural similarities between both monomers as both are aromatic rings

Received: December 7, 2021

Accepted: January 19, 2022

53 with two oppositely positioned carboxylic groups.^{9,10} In
54 addition, the FDCA bioproduction route is easily accessible
55 when compared to the challenging and inefficient TPA
56 bioproduction.^{11–14} The structures of both TPA and FDCA
57 are given in Scheme 1. When polymerized, aromatic polyesters

Scheme 1. Structures of Terephthalic Acid (TPA) and Furan-2,5-dicarboxylic Acid (FDCA)



58 produced from FDCA instead of TPA show very competitive
59 properties that are in some cases considered to be far superior
60 to TPA-based polyesters.^{15–19}

61 In general, semiaromatic polyesters are structurally designed
62 on the basis of both aliphatic and aromatic (co)monomeric
63 units. The incorporation of aromatic units into the polymer
64 structure helps increase the rigidity, hydrophobicity, and
65 thermal properties of the polymeric backbone, whereas the
66 aliphatic units in the form of aliphatic diacids or diols serve to
67 enhance the flexibility of the polymeric structure and lower its
68 glass transition temperature (T_g).^{20,21} Accordingly, the
69 combination of aliphatic and aromatic groups in semiaromatic
70 polyesters such as PET and PBT has shown a great
71 enhancement of properties and expanded the scope of their
72 applications, ranging from plastic bottles to synthetic fibers and
73 food packaging.^{22,23}

74 In recent years, many furan-based polyesters and polyamides
75 have been synthesized,^{21,24} and many research works have
76 focused on comparing them to their TPA-based counter-
77 parts.^{25–27} For example, via a two-step polycondensation
78 process in the presence of titanium isopropoxide ($\text{Ti}(\text{O}-i\text{-Pr})_4$)
79 as catalyst, Knoop et al.¹⁶ synthesized a series of polyethylene
80 furanoates (PEFs), polypropylene furanoates (PPFs), and
81 polybutylene furanoates (PBFs) with medium molecular
82 weights that are comparable to their TPA analogues and
83 show less coloration. Moreover, furan-based polyesters have
84 been shown to present enhanced gas barrier properties when
85 compared to their TPA counterparts.^{28,29} Regarding their
86 mechanical properties, PEF was found to be similar to PET in
87 terms of its Young's modulus and maximum stress values. In
88 contrast, PEF was shown to be significantly more brittle than
89 PET.³⁰ In another interesting study, the PBF ductility was
90 found to significantly increase as a function of the molecular
91 weight, reaching Young's modulus and elongation values
92 comparable to the reported values of commercial PBT when
93 the \bar{M}_n was $>16\,000\text{ g}\cdot\text{mol}^{-1}$. In contrast, lower values of
94 Young's modulus and elongation at break were reported when
95 the \bar{M}_n was $\sim 7000\text{ g}\cdot\text{mol}^{-1}$. This difference was suggested to
96 originate from the insufficient number of entanglements at
97 lower molecular weight values.¹⁷ Although FDCA-based
98 polyesters show great promising properties, they are still
99 prone to limitations, especially in regard to their fragility, slow
100 crystallization, and in some cases, poor biodegradability. To
101 address these issues, researchers have been trying to tune the
102 properties of FDCA-based polymers using an array of different

diols and diacids (cyclic, secondary, etc.).²¹ For example, the
incorporation of cyclic diols such as 1,4-cyclohexanedimethanol
along with propane-1,3-diol and FDCA has been shown to
increase the thermal stability of the polyesters produced.³¹
Moreover, the copolymerization of FDCA-based polyesters
such as PEF, PPF, and PBF with rigid cyclic diols such as 1,4-
cyclohexanedimethanol and 2,2,4,4-tetramethyl-1,3-cyclobuta-
nediol resulted in polymers with enhanced tensile strength yet
a lower elongation at break.^{32,33} Enzymatic catalysis has been
introduced as a greener synthetic approach toward the
production of polyesters, owing to its nontoxic nature, high
selectivity, and the possibility of processing under mild
conditions.^{34–36} When compared to current metal catalysts
used for polyester synthesis, they are advantageous by avoiding
any residual traces of harmful metals after synthesis and by
preventing any discoloration and side reactions that can occur
with metallic catalysis due to the elevated temperatures
required.³⁷ In addition, the high selectivity of some enzymes
can allow one to perform some reactions with minimal steps by
avoiding additional steps like protection/deprotection chem-
istries that would otherwise be required via these conventional
catalyses.^{38,39} Although the literature is rich in examples of
enzyme-catalyzed polyesterification to produce aliphatic
polyesters, the synthesis of aromatic polyesters remains less
studied mainly due to the need to use elevated reaction
temperatures when dicarboxylic aromatic (co)monomers are
used. Nevertheless, several promising attempts depicted in
multiple excellent review articles^{18,19} have been noted to
synthesize aromatic and semiaromatic polyesters via enzymatic
catalysis, which can be manageable at lower temperatures by
substituting diacid monomers with their methyl or ethyl diester
analogues. However, such polyesters were ill-defined with their
low molecular weights, mainly due to side reactions such as
ether formation as well as to the low temperature used, leading
to phase separation of the end-product and limited polymer
growth.^{40,41} In an attempt to overcome this limitation, Jiang et
al.³⁴ performed a two-step polycondensation reaction in
diphenyl ether using Novozym 435 (N435) as a catalyst,
which is a *Candida antarctica* lipase B (CALB) immobilized on
an acrylic resin. The results obtained showed that for the
polyesterification reaction between dimethyl furan-2,5-dicar-
boxylate (DMFDCA) and different aliphatic diols, specifically
hexane-1,6-diol, octane-1,8-diol, and decane-1,10-diol, at a
temperature of $140\text{ }^\circ\text{C}$, the polyesters obtained possessed a
high \bar{M}_n of 41 100, 41 000, and 51 600 $\text{g}\cdot\text{mol}^{-1}$, respectively.
However, the high temperature used significantly impacted the
activity of the recycled enzyme. Those values exceeded the
values obtained at $80\text{ }^\circ\text{C}$ by more than 10-fold. As enzymatic
catalysis proved to be better suitable for oligomer production,
several attempts to synthesize furan-based oligomers via
enzymatic catalysis have been made in recent years, where
different aromatic and semiaromatic oligomers were pro-
duced.^{42,43} Other attempts to synthesize semiaromatic diesters
via enzymatic catalysis were reported by Pellis et al.⁴⁴ Aliphatic
diols varying in chain length between C_4 – C_8 were reacted with
several aromatic monomers such as diethyl furan-2,5-
dicarboxylate, diethyl terephthalate, and diethyl isophthalate
in addition to different isomers of pyridine dicarboxylic acid.
The results showed that the reaction between 2,4-diethyl
pyridine dicarboxylate and octane-1,8-diol in diphenyl ether
led to the highest molecular weight ($\bar{M}_n = 14\,300\text{ g}\cdot\text{mol}^{-1}$). In
another research work, Pellis et al.⁴⁵ conducted the enzyme
catalyzed synthesis of furan and pyridine diol-based polyesters

166 such as 2,5-bis(hydroxymethyl)furan (2,5-BHMF), 3,4-bis-
167 (hydroxymethyl)furan (3,4-BHMF), and 2,6-bis-
168 (hydroxymethyl)pyridine using diphenyl ether as solvent. Via
169 a two-step polycondensation reaction maintained for 96 h at
170 85 °C, and apart from 3,4-BHMF polymers that gave low
171 yields and M_n , all reactions tested with varying chain-length
172 aliphatic diesters were successful with yields > 65% and M_n
173 reaching 5000 g·mol⁻¹.

174 Although semiaromatic polyesters such as PET and PBT or
175 their furan counterparts possess good physical properties, they
176 are resistant to biodegradation.^{46,47} To tackle this, semi-
177 aromatic terpolyesters such as polybutylene adipate tereph-
178 thalate (PBAT) were developed, consisting of aromatic and
179 aliphatic units and showing adequate mechanical properties
180 while being biodegradable at the same time.⁴⁸ In fact, the
181 biodegradation of such copolyesters was due to the presence of
182 aliphatic repeating units such as butylene adipate (BA) in
183 PBAT, which were more susceptible to hydrolysis and
184 microorganism attacks than the semiaromatic butylene
185 terephthalate (BT).^{48,49} In a study conducted by Herrera et
186 al.,⁵⁰ PBAT with an adipate/terephthalate ratio of 60/40 was
187 found to degrade at a faster rate than PBAT with a higher
188 terephthalate content (40/60). Such findings could allow for
189 adequate control over the properties and degradation time of
190 semiaromatic copolyesters such as PBAT simply by tuning the
191 adipate/terephthalate ratio. With the biodegradability advant-
192 age of such copolyesters, in addition to the advantages of
193 furan-based polyesters, researchers have been focusing in
194 recent years on developing furan-based copolyesters such as
195 polybutylene adipate furanoate (PBAF) aiming to produce
196 biobased polymers, which are also biodegradable and possess
197 adequate properties, allowing them to compete with TPA-
198 based polymers.^{51–56}

199 Although the enzymatically catalyzed synthesis of furan-
200 based polyesters such as PBF, among other types, was recently
201 reported in the literature,^{24,34,41} the enzymatic synthesis of
202 furan-based terpolyesters, on the other hand, is less studied.
203 Morales-Huerta et al.⁵⁷ synthesized poly(butylene furan-2,5-
204 dicarboxylate-co-succinate) via the ring-opening polymer-
205 ization of cyclic butylene furan-2,5-dicarboxylate and butylene
206 succinate oligomers yielding copolyesters with a \bar{M}_n ranging
207 between 16 000 and 31 000 g·mol⁻¹ where Novozym 435 was
208 loaded at 40% w/w relative to the totality of the concentration
209 of the monomers. On the other hand, the enzymatic
210 polycondensation approach toward semiaromatic copolyesters
211 was reported by Maniar et al.⁵⁸ by reacting DMFDCA and 2,5-
212 bis(hydroxymethyl)furan (BHMF) with aliphatic linear diols
213 and diacid ethyl esters. The highest \bar{M}_n determined for the
214 precipitated polymers was achieved when using 1,8-octanediol
215 and reached 16 000 g·mol⁻¹ after 72 h under vacuum with
216 temperature varying between 80 and 95 °C.

217 Previously, we introduced a statistical approach that allowed
218 us to predict the \bar{M}_n of poly(hexylene adipate) simply by
219 tuning the values of certain parameters such as vacuum,
220 enzyme loading, and temperature.⁵⁹ In our current work and
221 on the basis of the promising properties of furan-based
222 terpolyesters, such as their excellent mechanical properties and
223 biodegradability, we investigate the enzyme-catalyzed synthesis
224 of furan-based semiaromatic terpolyesters by reacting diethyl
225 furan-2,5-dicarboxylate (DEFDC) with variable aliphatic linear
226 dicarboxylic esters and primary diols. A special emphasis was
227 made on the influence of furan loading and the chain length of
228 the diols and diesters and how such factors can influence the

229 reactivity, molecular weight, and thermal properties of the end-
230 product. In addition, an amorphous fatty dimer diol, Pripol
2033, was tested for its influence on improving the reactivity in
231 the system where enzymatic catalysis was limited and its effect
232 on the thermal behavior of such polymers. Such polymers can
233 be used for applications in food packaging.
234

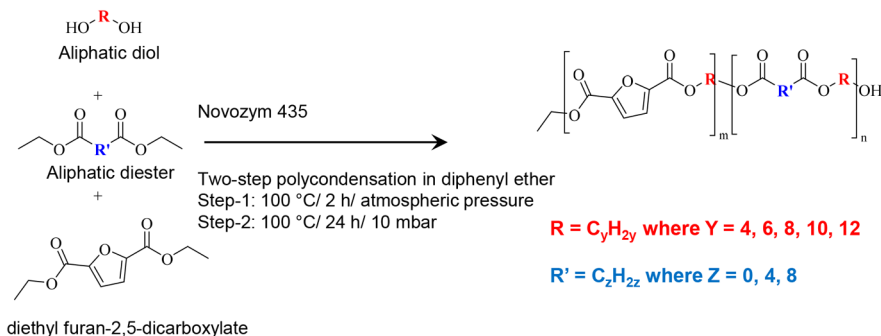
235 MATERIALS AND METHODS

Materials. Hexane-1,6-diol (97%), diethyl adipate (99%), sebacic
236 acid (99%), and diphenyl ether (99%) were purchased from Sigma-
237 Aldrich. Butane-1,4-diol (99%), octane-1,8-diol (98%), and dodecane-
238 1,12-diol (98%) were purchased from Acros Organics. Decane-1,10-
239 diol (97%) and diethyl oxalate were purchased from Alfa Aesar.
240 Furan-2,5-dicarboxylic acid (99.7%) was purchased from Satachem
241 Co. Pripol 2033 fatty dimer diol ((9Z,12Z)-18-[(6Z,9Z)-18-
242 hydroxyoctadeca-6,9-dienoxy]octadeca-9,12-dien-1-ol) (≥96.5) was
243 kindly provided by Croda Chemicals. Analytical grade methanol,
244 absolute ethanol, and chloroform (99%) were purchased from VWR.
245 All the reagents and solvents were used as received. Novozym 435
246 (N435), a *Candida antarctica* lipase B (CALB) immobilized on an
247 acrylic resin, was kindly provided by Novozymes. Chloroform D
248 (CDCl₃) (99.8%) and deuterated dimethyl sulfoxide (DMSO-*d*₆)
249 were purchased from Euriso-Top.
250

Synthesis of Diethyl Furan-2,5-dicarboxylate (DEFDC). In
251 general, 5 g of furan-2,5-dicarboxylic acid (FDCA) was added to 60
252 mL of absolute ethanol and 2 mL of sulfuric acid and refluxed
253 overnight under continuous stirring at 100 °C. The mixture was
254 allowed to cool, followed by evaporation to remove the excess amount
255 of ethanol. The solution was added dropwise into distilled water
256 under continuous stirring, resulting in FDCA precipitation. The
257 product was washed multiple times with distilled water before being
258 suspended in 100 mL of a H₂O solution, neutralized by adding 5%
259 NaCO₃, and finally filtered using a Buchner funnel under vacuum
260 application. The white crystalline powder obtained was dried
261 overnight under high vacuum, and the yield by weight achieved was
262 >75% w/w. ¹H NMR analysis confirmed the structure of diethyl
263 furan-2,5-dicarboxylate (DEFDC) with no detectable impurities; ¹H
264 NMR (CDCl₃, 300 MHz): δ 7.20 (s, 2H), 4.40 (q, *J* = 7.1 Hz, 4H),
265 1.39 (t, *J* = 7.1 Hz, 6H) ppm (see Figure S1).
266

**General Procedure for the Enzymatic Synthesis of Poly-
(alkylene alkanooate-co-alkylene furan-2,5-dicarboxylate).** *Ef-*
267 *fect of Diol Length (C₄ to C₁₂) and DEFDC Molar Ratio.* Furan-based
268 semiaromatic copolyesters were prepared by reacting DEFDC and
269 diethyl adipate with diols of different chain lengths varying from C₄
270 to C₁₂. As an example, the synthesis of poly(hexyleneadipate-co-
271 hexylene-2,5-furandicarboxylate) containing 50 mol % furan relative
272 to the total diesters was as follows: hexane-1,6-diol (4 mmol), diethyl
273 adipate (2 mmol), and DEFDC (2 mmol) were weighed and added
274 into a Schlenk tube. A predetermined amount (20% w/w) of N435
275 relative to the total weight of hexane-1,6-diol (4 mmol) and diethyl
276 adipate (4 mmol) was weighed and added to the mixture. Precisely, 1
277 mL of diphenyl ether (6.3 mmol) was added as the solvent of choice.
278 The reaction proceeded under atmospheric pressure for 2 h at 100 °C
279 (using an oil bath with continuous stirring kept constant at 350 rpm).
280 Afterward, the Schlenk tube was attached to a vacuum line, and the
281 pressure was decreased gradually within 1 h to reach a predetermined
282 value of 10 mbar to remove the byproduct (ethanol). The reaction
283 was left to proceed for 24 h; then, it was stopped by adding an excess
284 amount of chloroform under atmospheric pressure after a cooling
285 step, followed by direct filtration to remove the N435 beads. The
286 filtrate was then partially evaporated and then added dropwise to an
287 excess amount of cold methanol under stirring to precipitate the
288 obtained polymer. The mixture was then filtered, and the obtained
289 product was left to dry at room temperature for 24 h before being
290 collected and weighed. The percentage yield was calculated by
291 dividing the actual yield (816 mg) by the theoretical yield (932 mg).
292

Effect of Diester Length (C₂–C₆–C₁₀) and DEFDC Molar Ratio.
293 Following the same procedure as before, the influence of diester
294 length was examined by performing the copolymerization reaction
295

Scheme 2. Polycondensation Reaction of Variable Diols, Diethyl Adipate, and DEFDC in the Presence of N435 as Catalyst^a

^aWhere n varied between 4 and 12 depending on the diol used.

297 between hexane-1,6-diol and different chain-length diesters, specifi-
 298 cally diethyl oxalate (C_2), diethyl adipate (C_6), and diethyl sebacate
 299 (C_{10}), at variable DEFDC molar feed percent (0–90%). The same
 300 approach was used starting from dodecane-1,12-diol.

301 **Effect of Diol Length on DEFDC Conversion during Oligomeriza-**
 302 **tion: "A Comparison between Hexane-1,6-diol- and Dodecane-**
 303 **1,12-diol-Based Copolyesters".** In the first part of this study and
 304 following the same procedure as before, different samples containing
 305 either hexane-1,6-diol or dodecane-1,12-diol in addition to diethyl
 306 adipate and DEFDC were prepared by keeping an equimolar ratio
 307 between the diol and diesters while varying the DEFDC content from
 308 10% to 75%. The conversion of DEFDC into alkylene furanoate was
 309 monitored by withdrawing samples at different time intervals and
 310 exploiting the ^1H NMR signals at $\delta = 4.32$ – 4.34 of the methylene
 311 ($-\text{O}-\text{CH}_2-\text{C}_n\text{H}_{2n}-\text{CH}_2-\text{O}-$) of the alkylene furanoate, $\delta = 4.06$ –
 312 4.07 of the methylene ($-\text{O}-\text{CH}_2-\text{C}_n\text{H}_{2n}-\text{CH}_2-\text{O}-$) of the alkylene
 313 adipate, and $\delta = 3.65$ of the methylene ($\text{HO}-\text{CH}_2-\text{C}_n\text{H}_{2n}-\text{CH}_2-$
 314 OH) of the residual diol represented in eq S3. The X-furan amount
 315 (%) representing the evolution of furan content in the oligomers
 316 produced is given via eq S1

317 In the second part of this study, hexane-1,6-diol and dodecane-
 318 1,12-diol were added into the same reaction in equimolar amounts
 319 and reacted against 75% DEFDC and 25% of diethyl adipate while
 320 maintaining an equimolar ratio between the diols and diesters. The
 321 conversion of DEFDC into either hexylene furanoate or dodecylene
 322 furanoate was monitored via ^1H NMR in the same fashion as
 323 previously mentioned and by taking advantage of the global spectral
 324 deconvolution technique to distinguish between overlapping signals of
 325 hexylene furanoate and dodecylene furanoate. The aim was to
 326 monitor how two different chain-length diols could compete in the
 327 same reaction media.

328 **Effect of N435 % Loading.** Hexane-1,6-diol was chosen as a model
 329 monomer to see the effect of enzyme loading on the polymerization
 330 reaction. Similar to the general procedure mentioned above, hexane-
 331 1,6-diol was reacted with diethyl adipate and DEFDC at different
 332 molar percentages (10%, 25%, 50%, and 75%), and the N435 %
 333 loading was varied between 10% and 20% while maintaining similar
 334 reaction conditions.

335 **Effect of Fatty Dimer Diol (Pripol 2033).** The effect of Pripol 2033
 336 was tested in two experimental parts. In the first experimental
 337 approach, octane-1,8-diol and Pripol 2033 were reacted with DEFDC
 338 in equimolar (diol-diester) ratios (4 mmol). Pripol 2033 was added at
 339 10 and 20 mol % relative to the total diols in the reaction (or 13.7 and
 340 25 wt % relative to the total monomers), and the reactions proceeded
 341 for 2 h at 100 °C in 1 mL of diphenyl ether and 20% w/w N435
 342 loading, followed by 24 h under vacuum (10 mbar). The polyesters
 343 synthesized were compared in terms of conversion, X-furan, \bar{M}_n , and
 344 their thermal properties.

345 In the second experimental procedure, butane-1,4-diol and Pripol
 346 2033 were reacted against diethyl adipate (25 mol %) and DEFDC
 347 (75 mol %). Pripol 2033 was added at 10, 25, and 50 mol % relative to
 348 the diesters while maintaining an equimolar (diol-diester) ratio (4

mmol). The reactions proceeded for 2 h at 100 °C in 3 mL of 349
 diphenyl ether and 20% w/w N435 loading, followed by 72 h under 350
 vacuum (10 mbar). The synthesized polyesters were compared in 351
 terms of conversion, X-furan, \bar{M}_n , and their thermal properties. 352

353 **Analytical Methods. Nuclear Magnetic Resonance (NMR)**
 354 **Analysis.** The ^1H NMR spectra of the monomers and the recovered 354
 polymer were recorded at room temperature on a Bruker Avance 300 355
 instrument (delay time = 3 s, number of scans = 32) at 300.13 MHz 356
 using either CDCl_3 or $\text{DMSO}-d_6$ as solvents. Chemical shifts (ppm) 357
 are given in δ units and were calibrated using the residual signal of 358
 CDCl_3 and $\text{DMSO}-d_6$ at 7.26 and 2.5 ppm, respectively. Additionally, 359
 ^1H NMR was used to determine the furan content in the 360
 microstructure of the polymer, confirm conversion, and determine 361
 its rate (eqs S1, S2, and S3). DOSY spectra were recorded on an 362
 Avance II 400 Bruker spectrometer (9.4 T) regulated at 298 K in 363
 CDCl_3 and toluene- d_8 . Data acquisition and analysis were performed 364
 using Bruker TopSpin 3.2 and MestReLab 6.0. 365

366 **Gel Permeation Chromatography (GPC) Analysis.** Gel permea-
 367 tion chromatography (GPC) analysis was performed in chloroform 367
 as eluent (flow rate of 1 mL/min) at 23 °C using an Alliance e2695 368
 (Waters) apparatus and with a sample concentration of around 10–15 369
 mg/mL. A refractive index detector Optilab T-REX (Wyatt 370
 Technology) was used as a detector, and a set of columns, HR1, 371
 HR2, and HR4 (Water Styragel), was utilized. The molecular weight 372
 calibration curve was obtained using monodisperse polystyrene 373
 standards. 374

375 **Differential Scanning Calorimetry (DSC).** The thermal transition 375
 was recorded with differential scanning calorimetry (DSC) on a TA 376
 Discovery DSC 25 using a cooling–heating–cooling–heating 377
 method. First, samples of ~ 10 mg were sealed in aluminum pans; 378
 the temperature was equilibrated at -90 °C, followed by a heating 379
 ramp of 10 °C/min to 200 °C, then a cooling ramp of 10 °C/min to 380
 -90 °C, and a second heating ramp of 10 °C/min to 200 °C. The 381
 thermograms were analyzed using TA Instruments TRIOS software. 382

383 **Wide-Angle X-ray Scattering (WAXS).** Wide-angle X-ray scattering 383
 (WAXS) analysis were performed on a Xeuss 2.0 apparatus (Xenocs) 384
 equipped with a micro source using $\text{Cu K}\alpha$ radiation ($\lambda = 1.54$ Å) and 385
 point collimation (beam size: $500 \times 500 \mu\text{m}^2$). The sample to 386
 detector distance, around 15 cm, was calibrated using silver behenate 387
 as standard. Through view 2D diffraction patterns are recorded on a 388
 Pilatus 200k detector (Dectris). Integrated intensity profiles were 389
 computed from the 2D patterns using the Foxtrot software. The 390
 exposure time was 15 min. 391

RESULTS AND DISCUSSION

392
 393 Following the general procedure above, the polycondensation 393
 of different diols with diethyl adipate and DEFDC in the 394
 presence of N435 (see Scheme 2) was conducted in diphenyl 395
 ether, as it was previously reported to be the more suitable 396
 solvent to achieve high conversion and molecular weights.^{60–62} 397
 While maintaining the equimolarity between the diols and the 398

Table 1. Molecular Structure Analysis (X-furan), % Conversion, % Yield, \bar{M}_n , \bar{D}_M , and DP of Furan-Based Copolyesters with Variable Furan Content and Aliphatic Diols

entry	diol ^a	DEFDC feed (%) ^b	X-furan (%) ^c	conversion (%) ^d	yield by weight (%)	\bar{M}_n (g mol ⁻¹) ^e	\bar{D}_M ^f	DP ^g
1	C ₄	0	0	98	85	16 000	1.80	80
2	C ₄	10	12	86	68	4900	1.93	24
3	C ₄	25	27	95	62	1300	6.9	6
4	C ₄	50						
5	C ₆	0	0	97	91	9200	1.80	40
6	C ₆	10	12	95	77	9400	1.61	41
7	C ₆	25	27	98	82	11 100	2.13	48
8	C ₆	50	51	98	87	9600	2.09	41
9	C ₆	75	75	96	90	3800	1.91	16
10	C ₆	90	78	48	0			
11	C ₈	0	0	94	88	9000	1.94	35
12	C ₈	10	12	95	87	10 900	1.82	42
13	C ₈	25	27	95	86	8900	1.75	34
14	C ₈	50	49	91	74	9900	1.91	38
15	C ₈	75	75	96	84	7500	2.14	28
16	C ₈	90	87	96	87	4700	1.85	18
17	C ₁₀	0	0	95	98	9100	2.05	32
18	C ₁₀	10	12	95	93	8300	1.91	29
19	C ₁₀	25	27	95	92	8600	1.78	30
20	C ₁₀	50	50	94	83	10 300	1.84	35
21	C ₁₀	75	74	95	92	7300	2.04	35
22	C ₁₀	90	89	97	99	8500	2.27	29
23	C ₁₂	0	0	95	98	7700	2.07	25
24	C ₁₂	10	11	95	97	9900	2.01	31
25	C ₁₂	25	26	96	93	9700	2.21	31
26	C ₁₂	50	50	95	95	8700	1.97	27
27	C ₁₂	75	74	95	89	6300	1.98	20
28	C ₁₂	90	88	97	100	7300	2.19	23

^aC₄ = butane-1,4-diol, C₆ = hexane-1,6-diol, C₈ = octane-1,8-diol, C₁₀ = decane-1,10-diol, and C₁₂ = dodecane-1,12-diol. ^bDEFDC feed (%) represents the molar percentage of diethyl 2,5-furandicarboxylate added, relative to the total diester amount. ^cX-furan (%) is defined as the molar fraction of the alkylene furan-2,5-dicarboxylate repeating unit in the copolymer and determined via ¹H NMR per eq S1. ^dConversion (expressed in %) represents the total amount of reacted diols relative to the overall diols in the system and was calculated by ¹H NMR via eq S2. ^eThe number-average molecular weight (\bar{M}_n) was obtained from GPC analyses (CHCl₃, 23 °C, polystyrene standards). \bar{M}_n values might be skewed to higher values for longer chain comonomers. ^fMolar mass dispersity ($\bar{D}_M = \bar{M}_w/\bar{M}_n$) was obtained from GPC analyses (CHCl₃, 23 °C, polystyrene standards). \bar{D}_M might be skewed to lower values due to fractionation (precipitation). ^gDP (degree of polymerization) = \bar{M}_n/M_0 , where M_0 is the molecular weight of the repeating unit.

399 diesters, the molar percent of DEFDC relative to the aliphatic
400 diester was varied between 0 and 90%. Different aliphatic diols
401 tested as (co)monomers were butane-1,4-diol, hexane-1,6-diol,
402 octane-1,8-diol, decane-1,10-diol, and dodecane-1,12-diol.

403 The impact of the diol length and furan content on the final
404 copolymer properties were both assessed in terms of
405 copolymer composition (X-furan), total conversion (%),
406 yield by weight (%), \bar{M}_n , dispersity (\bar{D}_M), and degree of
407 polymerization (DP) (Table 1). Peak assignments and the
408 respective calculations are given in Figure S2 and eqs S1 and
409 S2.

410 From Table 1, it was observed that the increase in DEFDC
411 content had a negative impact on X-furan, conversion, yield,
412 \bar{M}_n , and DP of copolymers synthesized from shorter diols. The
413 maximum quantities of furan successfully incorporated into
414 copolymers based on butane-1,4-diol and hexane-1,6-diol were
415 27 and 75 mol %, achieving yields of 62% and 90% (as
416 observed in entries 3 and 9), respectively. The increase of the
417 feed molar percentage of DEFDC with these short diols
418 limited the copolymer growth and led to a failure in
419 precipitation, which was assumed to result from the low
420 reactivity and the formation of short oligoesters that did not
421 precipitate in methanol. No detectable conversion or yield was

observed (see entry 4) when the DEFDC feed was increased to 422
50%, while only 48% conversion was calculated when the 423
DEFDC feed was increased to 90% (as observed in entry 10) 424
without any detectable yield. Similarly, the DP of the 425
copolymers prepared with butane-1,4-diol was highly influ- 426
enced by DEFDC feed, where increasing the DEFDC feed by 427
only 10% led to a drop in DP from 80 (entry 1) to 24 (entry 2) 428
and further decreased to 6 (entry 3) with 25% DEFDC. On the 429
other hand, copolymers based on octane-1,8-diol, decane-1,10- 430
diol, and dodecane-1,12-diol showed a stable conversion 431
(>90%) and high yields without any noticeable variations as 432
a function of the DEFDC feed increase. The DP of the 433
copolymers based on octane-1,8-diol was partially affected at 434
high DEFDC content, decreasing from 38 to 28 to 18 with the 435
increase in DEFDC feed from 50% to 75% to 90%. Longer 436
diols were not significantly affected by the increase in DEFDC 437
feed %, where copolymers based on decane-1,10-diol and 438
dodecane-1,12-diol maintained a relatively stable DP at high 439
DEFDC feed. The formation of poly(alkylene alkanoate-co- 440
alkylene furan-2,5-dicarboxylate) rather than poly(alkylene 441
alkanoate) and poly(alkylene furan-2,5-dicarboxylate) homo- 442
polymers was confirmed by performing DOSY NMR scans. 443
The spectrum provided in Figure S3 shows a single diffusion 444

445 coefficient for the produced poly(dodecylene adipate-co-
446 dodecylene furan-2,5-dicarboxylate) representing entry 26.

447 What was generally noticed from these results is that the
448 limitation imposed by the increase in DEFDC feed became less
449 significant as a function of the increase in the diol length,
450 where up to 90% DEFDC was successfully incorporated into
451 the copolyesters based on octane-1,8-diol, decane-1,10-diol,
452 and dodecane-1,12-diol. The superior catalytic efficiency of
453 N435 or CALB catalysts toward longer diols in the presence of
454 high furan content agreed well with the previously documented
455 results by Jiang et al.³⁴ They suggested that, besides the better
456 selectivity of CALB toward longer diols, furan-based polyesters
457 based on longer diols showed higher solubility in the reaction
458 media (diphenyl ether) and lower melting points compared to
459 those produced from shorter diols, which precipitated rapidly
460 due to the reasons mentioned above and prevented polymer
461 growth. In another study, Bazin et al.⁶³ assumed that the
462 limited polymer growth detected in terpolymers synthesized in
463 diphenyl ether based on hexane-1,6-diol, diethyl adipate, and
464 dimethyl furan-2,5-dicarboxylate was mainly a solubility
465 limitation, rather than a catalytic one, where high furan
466 content (90%) leads to early precipitation and limited polymer
467 growth. Surprisingly though, in our work, and contrary to
468 previous results in the literature (performed under similar
469 conditions in diphenyl ether or bulk),⁶¹ an increase in the diol
470 length in the absence of DEFDC did not seem to cause any
471 increase in the DP of the corresponding aliphatic polyesters.
472 On the contrary, the polymer based on butane-1,4-diol and
473 diethyl adipate (entry 1) was found to possess the highest DP
474 (80) among the aliphatic polyesters, while the DP was
475 maintained within a range of 25–40 for polymers based on
476 hexane-1,6-diol (entry 5), octane-1,8-diol (entry 11), decane-
477 1,10-diol (entry 17), and dodecane-1,12-diol (entry 23).
478 However, it should be noted that the limitations in polymer
479 growth could have stemmed from the diminishing mixing
480 speed due to the increase in the viscosity of the samples, which
481 might have posed a negative effect on the heat and mass
482 transfer. In fact, it was observed that the mixing efficiency
483 decreased rapidly in the reactions containing long diols, while
484 it took more time to notice the same decrease when shorter
485 diols were used. This observation could further justify the
486 limited DP values with long diols.

487 The influence of the diester length was examined by
488 comparing 1,2-diethyl oxalate (C_2), 1,6-diethyl adipate (C_6),
489 and 1,10-diethyl sebacate (C_{10}). The results showing the
490 evolution of DP as a function of diester length are given in
491 Figure 1, and further results concerning the X-furan,
492 conversion (%), yield (%), \bar{M}_n (g mol^{-1}), \bar{D}_M , and DP are
493 stated in Table S1.

494 With the exception of 1,2-diethyl oxalate that did not yield
495 any polymers when reacted against hexane-1,6-diol, the
496 increase in the diester length from C_6 to C_{10} did not have a
497 significant impact on the molecular weight of the copolymers
498 produced, as observed in Figure 1a. On the other hand, in
499 Figure 1b, the reaction of dodecane-1,12-diol with diethyl
500 oxalate (C_2) in the presence or absence of DEFDC led to
501 copolymers with a DP ranging between 26 and 34. The DP
502 decreased on average with an increase in the diester length
503 down to a DP of 20–31 with diethyl adipate (C_6) and a further
504 decrease in DP down to 10–18 with diethyl sebacate (C_{10}).
505 However, as mentioned before, the decrease in DP with longer
506 diesters could have resulted from the high viscosity built up in
507 the system that could have limited polymer growth. Moreover,

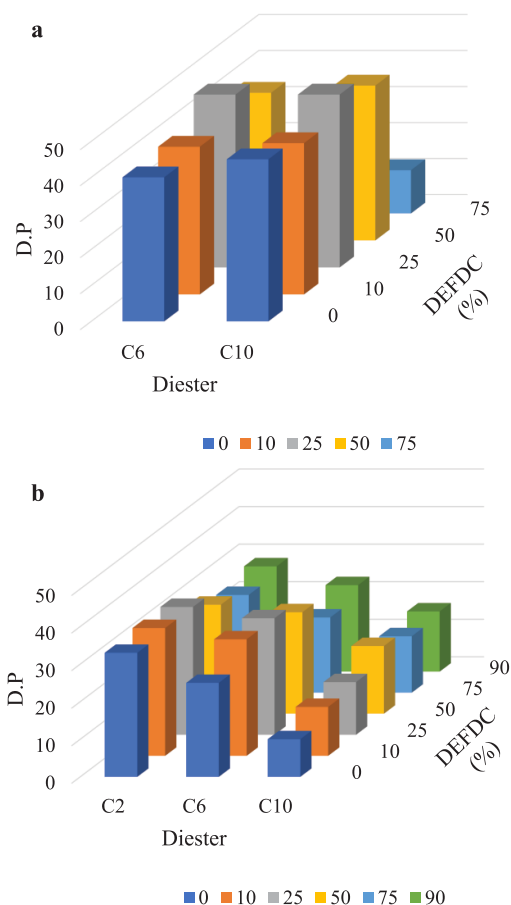


Figure 1. (a) Variation in DP of furan-based copolyesters with variable furan content based on hexane-1,6-diol and different aliphatic diesters. (b) Variation in DP of furan-based copolyesters with variable furan content based on dodecane-1,12-diol and different aliphatic diesters, where C_2 = 1,2-diethyl oxalate, C_6 = 1,6-diethyl adipate, and C_{10} = 1,10-diethyl sebacate.

508 unlike copolyesters based on hexane-1,6-diol, copolyesters
509 based on dodecane-1,12-diol and regardless of the aliphatic
510 diester used did not show significant variations in terms of
511 conversion, yield, and DP as a function of increasing the
512 DEFDC feed.

513 Taking advantage of the difference in reactivity between
514 different chain-length diols, a time course study was performed
515 comparing hexane-1,6-diol and dodecane-1,12-diol in terms of
516 conversion during the oligomerization step as a function of
517 DEFDC content in the feed. The results showing the evolution
518 of conversion in addition to X-furan representing the furan
519 content (%) in the produced oligomers are given in Figure 2.

520 From Figure 2, the reactions of two diols showed similar
521 time course profiles at 10% and 25% DEFDC in the feed,
522 where in both cases, the conversion representing the total
523 amount of diols that reacted with DEFDC reached within a 2 h
524 interval a constant value of 6% with C_6 (10%) and C_{12} (10%)
525 and 14% with C_6 (25%) and C_{12} (25%). Similarly, the amount
526 of furan (X-furan) in the copolymer structure was similar to
527 both diols reaching 10% with C_6 (10%) and C_{12} (10%) and
528 25% with C_6 (25%) and C_{12} (25%), respectively. Such values
529 accurately represented the DEFDC in the feed. However, as
530 the DEFDC feed content increased to 50% and 75%, variations
531 in terms of conversion and X-furan were observed when
532 comparing hexane-1,6-diol to dodecane-1,12-diol-based oli-

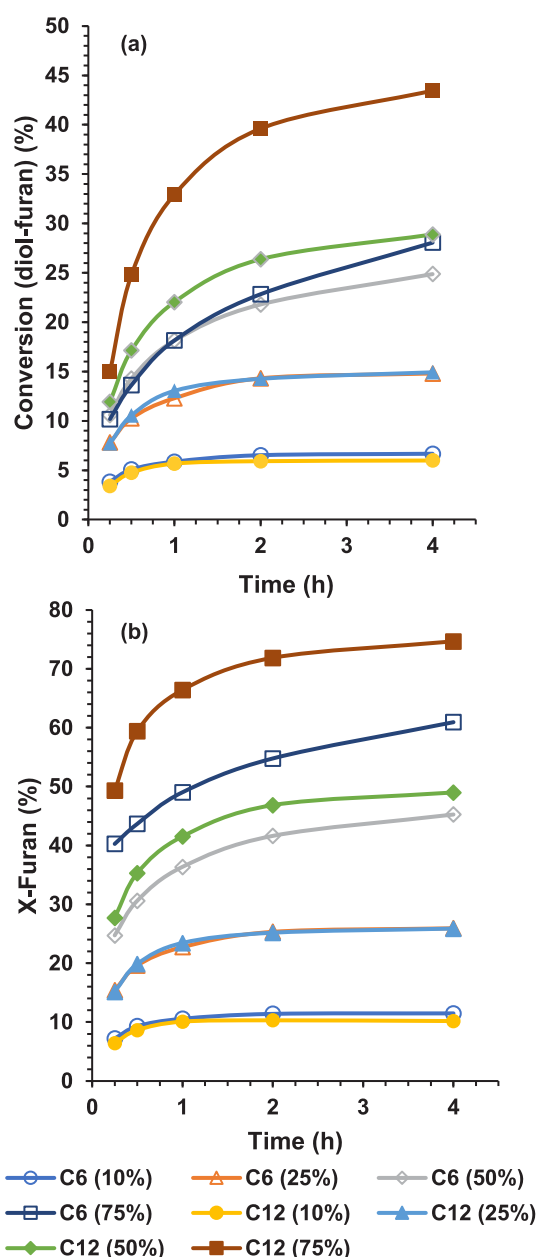


Figure 2. (a) Conversion of diols to furan-esters (expressed in mol %) during oligomerization, determined via ^1H NMR. Medium: diphenyl ether; N435: 20% w/w; temperature: 100 $^\circ\text{C}$. (b) Composition of copolyesters during oligomerization showing the evolution of furan content in the produced oligomers determined via ^1H NMR. Medium: diphenyl ether; N435: 20% w/w; temperature: 100 $^\circ\text{C}$.

533 goesters, where at 50% DEFDC feed content, the conversion
 534 calculated for C_6 (50%) and C_{12} (50%) reached values of 25%
 535 and 29% and the X-furan values were 45% and 49%,
 536 respectively. The superior reactivity of dodecane-1,12-diol
 537 with DEFDC was further confirmed at higher DEFDC content
 538 (75%), where for C_6 (75%), conversion did not increase
 539 beyond 29% after 4 h of oligomerization time compared to
 540 43% with C_{12} (75%) within the same time limit. Similarly, the
 541 X-furan was limited to 61% with C_6 (75%) but was equivalent
 542 to the DEFDC feed percentage with C_{12} (75%) with a X-furan
 543 value of 75%. These results further confirmed the results
 544 obtained in Table 1, suggesting that, in the presence of N435
 545 as a catalyst, longer diols were more reactive toward DEFDC

546 than their shorter counterparts. However, at low DEFDC
 547 content (<25%), and in the presence of diethyl adipate, the
 548 conversion of both seemed to proceed at a very similar rate
 549 regardless of the diol length.

550 As the reactivity differences between hexane-1,6-diol and
 551 dodecane-1,12-diol appeared to be more significant in the
 552 presence of high amounts of DEFDC, another time course
 553 study was performed to compare hexane-1,6-diol and
 554 dodecane-1,12-diol reactivity using the same system as detailed
 555 under the Materials and Methods. The evolution of X-furan
 556 and X-adipate for both hexane-1,6-diol and dodecane-1,12-diol
 557 is given in Figure S4.

558 It was evident from Figure S4 that, after only 15 min from
 559 the start of the reaction, the oligoester structures were
 560 dominated by hexanediol-adipate and dodecanediol-adipate
 561 ester units recording 32% and 36%, respectively, relative to the
 562 total esters formed in the system, while hexanediol-furan and
 563 dodecanediol-furan esters were limited to 13% and 19%,
 564 respectively. The domination of diol-adipate esters during the
 565 first minutes of the reaction resulted from the higher reactivity
 566 of diols toward aliphatic diesters under N435 mediated
 567 catalysis. As the reaction proceeded, the X-adipate for both
 568 diols started to decrease gradually while the X-furan increased
 569 simultaneously, where after 4 h, X-adipate(hexane-1,6-diol)
 570 and X-adipate(dodecane-1,12-diol) decreased to reach values
 571 of 13% and 18%, whereas the X-furan(hexane-1,6-diol) and
 572 X-furan(dodecane-1,12-diol) increased to reach 33% and 37%,
 573 respectively. Unlike what was observed in Figure 2 in the case
 574 of hexane-1,6-diol, where the X-furan was limited to 61% after
 575 4 h, the presence of the two diols in the same system allowed
 576 the oligoesters' composition to rearrange as the reaction
 577 proceeded to reach, after 4 to 6 h, a composition that
 578 accurately represents the feed ratio of diols and esters based on
 579 the summation of X-furan of both hexane-1,6-diol and
 580 dodecane-1,12-diol.

581 These two time course studies showed how N435 showed
 582 minimal catalytic differences between hexane-1,6-diol and
 583 dodecane-1,12-diol at low DEFDC content, which is evident
 584 from the conversion profiles presented in Figure 2. On the
 585 other hand, it was also clear how, in the presence of an
 586 aromatic group such as DEFDC, N435 tended to catalyze the
 587 transesterification reaction between dodecane-1,12-diol and
 588 DEFDC at a faster rate compared to similar reactions with
 589 hexane-1,6-diol. These observations suggest that, in enzymatic
 590 catalysis based on N435, longer diols are better suitable to
 591 react against high furan content.

592 The impact of % w/w N435 loading was tested by
 593 comparing the polycondensation reaction of hexane-1,6-diol
 594 with diethyl adipate and DEFDC at 10 and 20% w/w N435
 595 enzyme loading. The results in Table S2 showed modest
 596 variations in the results at low DEFDC % (entries 22' and
 597 26'). However, as the DEFDC feed content increased, it
 598 became evident that a higher enzyme loading was necessary to
 599 conduct the reaction, where copolymers based on 10% N435
 600 (see entries 24' and 25' in Table S2) had a minute amount of
 601 furan in their structures (3–4%) and a low conversion of 24
 602 and 17%, respectively. While elevated conversions and yields
 603 were persistent in copolymers based on 20% N435 loading.

604 As the reactivity of diols and the M_n of the copolyesters
 605 tended to decrease with high amounts of DEFDC, especially
 606 with shorter diols, small amounts of Pripol 2033 were
 607 incorporated in the reaction media as mentioned in the
 608 Materials and Methods and observed in Scheme 3 in an

Scheme 3. Enzyme-Catalyzed Polycondensation Reaction of Octane-1,8-diol, Pripol 2033, and DEFDC

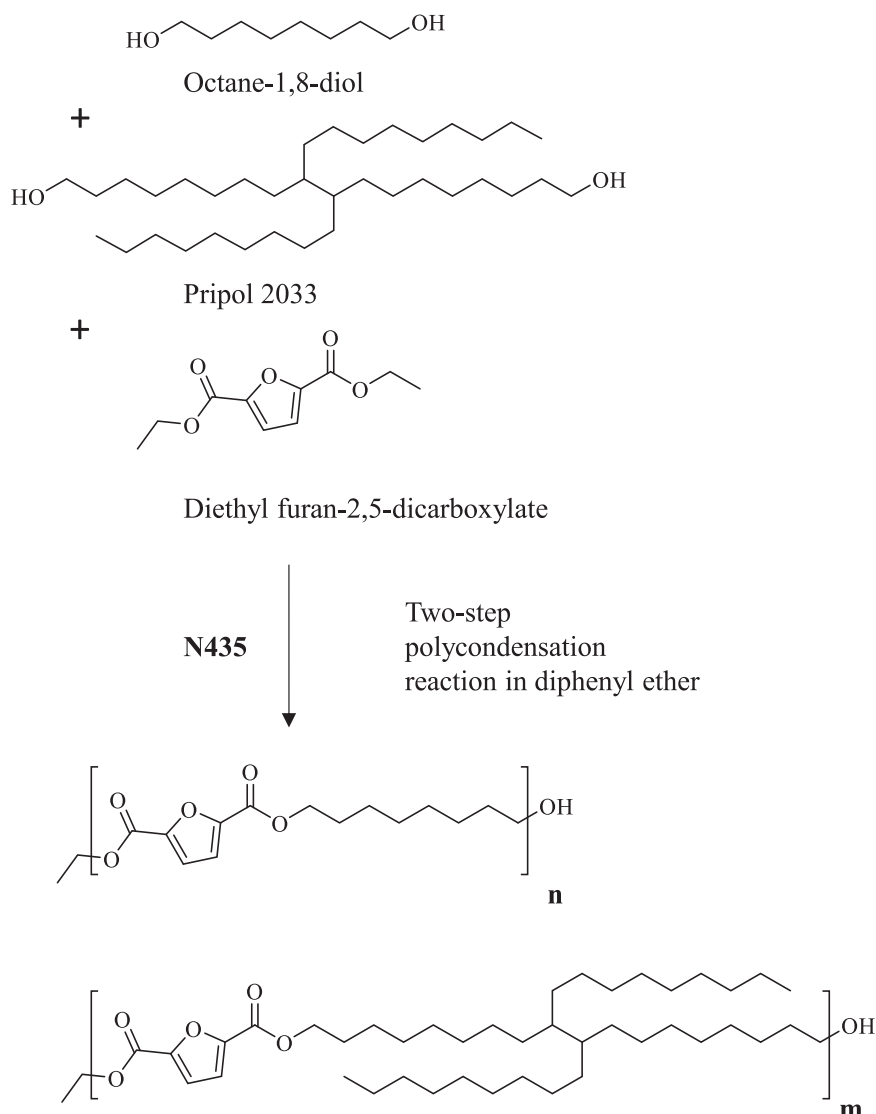


Table 2. X-furan, % Conversion, % Yield, and \bar{M}_n of Copolyesters Based on Butane-1,4-diol and DEFDC with or without Pripol 2033

entry	Pripol 2033 (%) ^a	X-furan (1,4-BD) (%) ^b	X-furan (Pripol) (%) ^c	X-furan (total) (%) ^d	conversion (%) ^e	yield by weight (%)	\bar{M}_n (g mol ⁻¹) ^f
29	0	0	0	0			
30	10	0	0	0			
31	25	56	19	75	99	88	7700
32	50	37	38	75	99	91	12 000

^aPripol 2033 (%) represents the molar percentage of Pripol 2033 added, relative to the total diester amount. ^bX-furan (1,4-BD) (%) = molar percent of the butylene furandicarboxylate unit in the copolymer, calculated via eq S1. ^cX-furan (Pripol) (%) = molar percent of the Pripol-furandicarboxylate unit in the copolymer, calculated via eq S1. ^dX-furan (total) (%) = molar percent of the alkylene furandicarboxylate unit in the copolymer, equal to the summation of X-furan (1,4-BD) and X-furan (Pripol). ^eConversion (expressed in %) is calculated via ¹H NMR using eq S2. ^fThe number-average molecular weight (\bar{M}_n) is obtained from GPC analyses (CHCl₃, 23 °C, polystyrene standards).

609 attempt to overcome the limitations of producing copolyesters
610 with high aromatic content via enzymatic catalysis.

611 As observed in Table S3, the yield by weight and M_n
612 increased significantly with the addition of Pripol 2033 from
613 68% and 2700 g·mol⁻¹ up to 90% and 5300 g·mol⁻¹ upon the
614 addition of 10% and 20% of Pripol 2033 relative to DEFDC.
615 The formation of a single copolyester rather than two
616 homopolymers was confirmed by performing a DOSY NMR

analysis for entry 32'; the spectrum showing a single diffusion
617 coefficient for the concerned peaks is provided in Figure S5. 618

619 As semiaromatic copolyesters based on small diols such as
620 butane-1,4-diol were limited to small amounts of DEFDC
621 (~25%) and to small molecular weights and yields, Pripol
622 2033 was used in a similar approach as before to enhance the
623 polycondensation reaction in the presence of butane-1,4-diol.
624 The reactions proceeded as observed in Scheme S1 in
625 equimolar ratios between the diols and the diesters, where

626 Pripol 2033 was added at 10%, 25%, and 50% relative to the
 627 diesters. Similar to what was observed before in the case of
 628 butane-1,4-diol at high DEFDC loading and even after
 629 extending the reaction time to 72 h and increasing the volume
 630 of diphenyl ether up to 3 mL to avoid mixing issues, butane-
 631 1,4-diol did not react with DEFDC when the latter was added
 632 at 75% relative to the total diesters in the reaction, and no
 633 copolyesters were collected (entry 40, Table 2). In fact, the ^1H
 634 NMR of the sample collected from the reaction media after 72
 635 h did not show any peaks representing the formation of an
 636 ester bond between butane-1,4-diol and DEFDC. The same
 637 observation continued upon the addition of 10% Pripol 2033
 638 (entry 41, Table 2) with no detected changes in the reactivity
 639 toward DEFDC whether for butane-1,4-diol or for Pripol 2033.
 640 However, upon a further increase in Pripol 2033 molar loading
 641 up to 25%, the X-furan detected in the ^1H NMR sample was
 642 equivalent to the DEFDC molar feed percent (75%) with 56%
 643 resulting from the esterification of butane-1,4-diol and DEFDC
 644 and 19% of Pripol 2033 and DEFDC and a high conversion of
 645 $\sim 99\%$ (entry 42, Table 2). Likewise, when butane-1,4-diol and
 646 Pripol 2033 were in equimolar amounts, the reaction
 647 proceeded to reach a high conversion, and the X-furan reached
 648 75% divided equally between butane-1,4-diol and Pripol
 649 2033 (entry 43, Table 2). The increase in the Pripol 2033
 650 feed ratio had a positive impact on reactivity, and as a result, a
 651 higher \bar{M}_n was achieved, reaching 7700 and 12 000 $\text{g}\cdot\text{mol}^{-1}$
 652 with 25% and 50% Pripol 2033.

653 The DSC profiles of the prepared polymers were determined
 654 following the protocol stated in the Materials and Methods.
 655 The results given in Figure 3 representing the entries in Table
 656 1 showed the evolution of major melting endotherms (T_m) and
 657 crystallization enthalpies (ΔH_m) during the second heating
 658 cycle as a function of DEFDC molar ratio and diol length. For

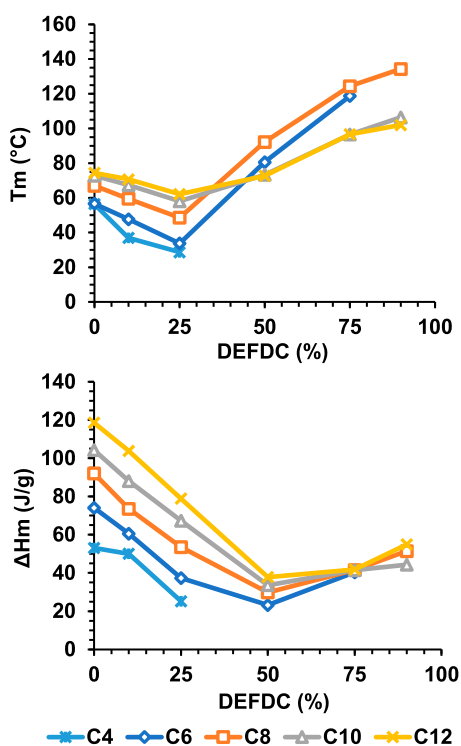


Figure 3. Variations in melting endotherms ($^{\circ}\text{C}$) and crystallization enthalpies (J/g) as a function of diol length and furan content.

up to 25 mol % DEFDC feed, the melting endotherms of the
 copolymers showed a gradual decrease as a function of the
 increase in DEFDC molar content, where longer diols showed
 higher melting endotherms. However, as the DEFDC content
 increased beyond 25 mol %, the melting endotherms started
 increasing. Copolymers based on hexane-1,6-diol showed an
 increase in their melting endotherms from 34 $^{\circ}\text{C}$ at 25 mol %
 DEFDC up to 81 and 119 $^{\circ}\text{C}$ at 50 and 75 mol % DEFDC
 content. Similarly, copolymers based on octane-1,8-diol
 showed a similar increase in their melting endotherms
 exceeding that of hexane-1,6-diol based copolymers, where
 T_m increased from 49 $^{\circ}\text{C}$ at 25 mol % DEFDC up to 92, 124,
 and 134 $^{\circ}\text{C}$ for 50, 75, and 90 mol % DEFDC feed ratios.
 Although the increase in DEFDC molar content also resulted
 in a positive shift in the melting endotherms of copolymers
 based on C_{10} and C_{12} diols, this increase was not as significant
 as those for shorter diols. It should be noted that copolymers
 based on C_8 , C_{10} , and C_{12} diols showed a second but minor
 melting endotherm at 50 mol % DEFDC, which appeared to
 fall within close proximity to the main endothermic peaks,
 suggesting the coexistence of two crystalline structures. In fact,
 the thermal behavior of these copolyesters represented in
 Figure 3 and showing a decrease followed by an increase in the
 melting endotherms and the coexistence of two crystalline
 phases at certain molar ratios suggest a pseudoeutectic
 behavior and isodimorphic cocrystallization.^{64,65} The crystal-
 lization enthalpy, which was higher for aliphatic copolymers
 based on longer diols, showed a gradual decrease as a function
 of DEFDC feed ratio until reaching a transitional point (~ 50
 mol % DEFDC), followed by an increase upon further DEFDC
 addition ($>50\%$ DEFDC). In fact, the pseudoeutectic point in
 copolymers that is usually characterized by the coexistence of
 two crystalline phases and represents the minimal crystalline
 value usually falls around equimolar monomer ratios, but it can
 vary according to the nature of the repeating unit.^{64,66} The
 different crystal phases were later confirmed via WAXS
 analysis.

Regarding the glass transition temperature (T_g), Table S4
 depicts its evolution as a function of diol length and DEFDC
 molar content. Due to the high crystallinity in some samples,
 the T_g was not detected in all copolyesters. As observed in
 Table S4, the T_g appeared to increase as a function of
 increasing DEFDC mol % with all tested copolymers, but no
 specific pattern that relates the length of the tested diols to the
 value of T_g was observed. During the first heating cycle and at
 50 mol % DEFDC feed, the polymer based on C_6 (entry 8)
 showed a glass transition temperature at -47 and a premelting
 point at 43 $^{\circ}\text{C}$, belonging to adipate-rich and furan-rich blocks,
 respectively. However, during the second heating cycle, the
 premelting point at 43 $^{\circ}\text{C}$ disappears and only a T_g at -40 $^{\circ}\text{C}$
 is observed. The same observation was noticed at 75 mol %
 DEFDC (entry 9). Similarly, polymers based on C_8 diol
 showed a similar behavior at 50 and 75 mol % DEFDC feed
 (entries 14 and 15), but at 90 mol % DEFDC (entry 16), only
 a premelting point at 45 $^{\circ}\text{C}$ appeared during the first heating
 cycle, while no changes were observed during the second
 heating cycle. The polymers based on C_{10} diol showed a T_g of
 -44 and -35 $^{\circ}\text{C}$ at 50 and 75 mol % DEFDC during the
 second heating cycle, while polymers based on C_{12} did not
 show any T_g with 75 and 90 mol % DEFDC (entries 27 and
 28). What was noticeable from these results was that, although
 changes in the melting endotherms as a function of furan
 content were observed for all copolymers, their change was

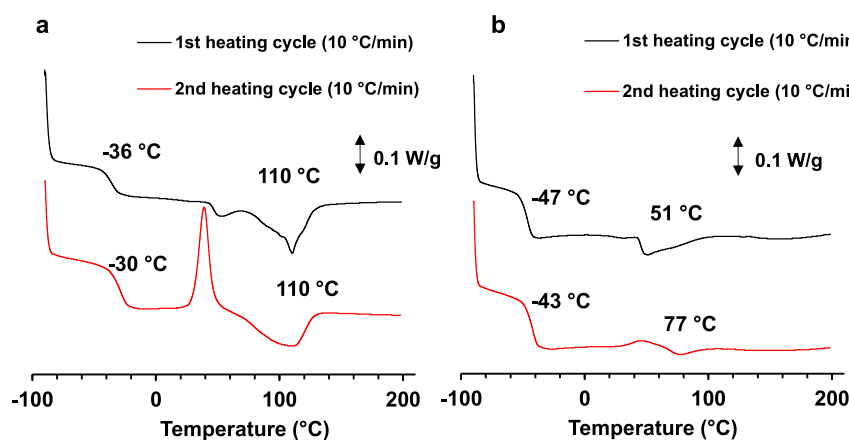


Figure 4. DSC profiles of entries 31 (a) and 32 (b) showing the first and second heating cycle.

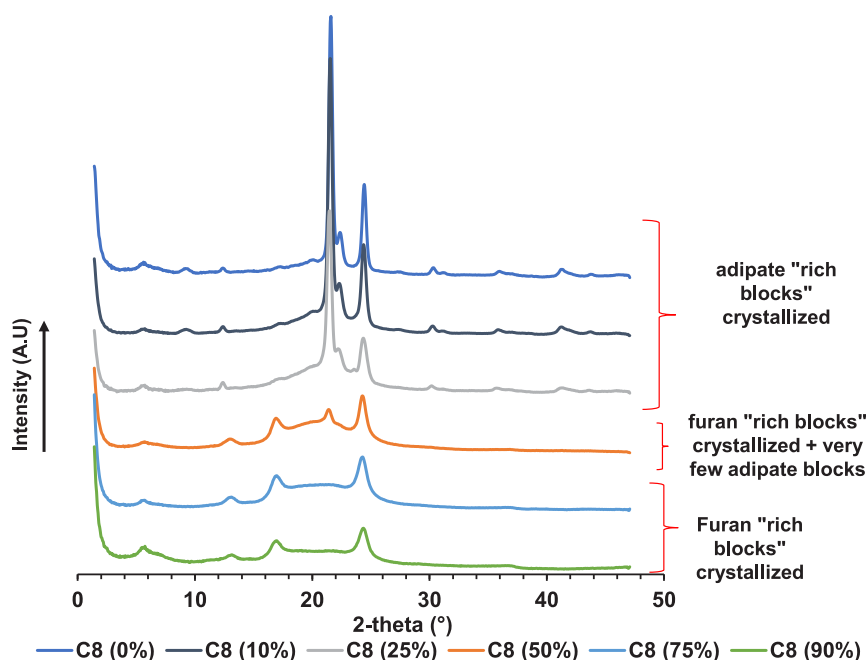


Figure 5. WAXS profiles of poly(octyleneadipate-co-octylenefuranoate) as a function of increasing the DEFDC content.

722 more pronounced with copolymers based on shorter diols
 723 achieving higher T_m values at high DEFDC content, which is in
 724 agreement with previous reports in the literature associating
 725 the decrease in T_m to the increase in the number of methylene
 726 groups.^{10,34} Regarding the influence of diester length on the
 727 DSC profiles of the copolymers produced, Figure S6 shows the
 728 evolution of both the melting endotherms and crystallinity as a
 729 function of both DEFDC mol % and diester length. The
 730 increase in mol % DEFDC showed a similar effect on the DSC
 731 profiles as what was observed in Figure 3. However, no direct
 732 relation was found relating the evolution of the DSC profiles as
 733 a function of the diester length.

734 Regarding the thermal properties of the copolyesters based
 735 on Pripol 2033, octane-1,8-diol, and DEFDC depicted in
 736 Scheme 3 and during the second heating cycle (see Table S3),
 737 all polymers showed an endothermic peak that gradually
 738 decreased as a function of increasing Pripol 2033 content from
 739 140 °C in entry 30' in the absence of Pripol 2033 down to 135
 740 and 129 °C with 10% and 20% Pripol 2033, respectively.
 741 Similarly, the crystallinity also decreased from 66 to 38 J/g.

The incorporation of Pripol 2033 at 25% along with butane- 742
 1,4-diol, diethyl adipate, and DEFDC as depicted in Table 2 743
 resulted in a highly viscous yellow sticky liquid, which during 744
 the first heating cycle of the DSC (Figure 4), the copolymer 745 f4
 given in entry 31, showed a T_g at -36 °C and a broad melting 746
 endotherm peaking at 110 °C with an enthalpy of 16 J/g. The 747
 cooling cycle did not show any recrystallization peaks. During 748
 the second heating cycle, the first T_g increased by 6 °C up to 749
 -30 °C, followed by a cold crystallization peak at 39 °C. The 750
 T_m peaked at 109 °C with a slight decrease in enthalpy from 16 751
 to 12 J/g. The decrease in crystallinity might have risen from 752
 the incomplete crystallization during the second heating cycle 753
 and the close proximity between the crystallization and melting 754
 point. Regarding entry 32, the increase in Pripol 2033 feed to 755
 50 mol % led to the formation of a copolyester with a T_g 756
 appearing at -47 °C during the first heating cycle and a T_m at 757
 51 °C with an enthalpy not exceeding 5.5 J/g. During the 758
 second heating cycle, the T_g shifted slightly toward 43 °C, 759
 followed by a cold crystallization peak at 46 °C. Directly after 760
 crystallization, the T_m peaked at 77 °C with minimal enthalpy 761
 that did not exceed 1 J/g. The big shift in the T_m peak from 51 762

763 °C during the first heating cycle to 77 °C on the second cycle
764 could have resulted from the presence of the cold
765 crystallization and the melting peaks in very close quarters,
766 masking any melting that might have occurred at similar
767 intervals. The copolymer in entry 32 appeared as a white
768 flexible film. The decrease in T_g as a function of increasing
769 Pripol 2033 content reflects an increase in the flexibility of the
770 polymer structure and increases the distance between the rigid
771 blocks, which subsequently decreases the crystallinity and the
772 crystallization rate.⁶⁷

773 To further study the influence of the DEFDC molar content
774 and diol length on the crystallinity of the copolymers, wide-
775 angle X-ray scattering (WAXS) was employed following the
776 protocol stated in the [Materials and Methods](#). Regarding the
777 influence of DEFDC feed %, copolymers based on octane-1,8-
778 diol with DEFDC content varying between 0 and 90% were
779 examined and compared (see [Figure 5](#)). For C_8 (0%), the
780 WAXS profile was dominated by two major peaks at 22° and
781 25°, which appeared to be very similar to the profiles of similar
782 aliphatic polymers tested in the literature such as the case of
783 poly(hexylene succinate).⁶⁸ For up to 25% DEFDC feed, the
784 crystallinity continued to be dominated by poly(octylene
785 adipate) crystals. However, upon the increase in DEFDC to
786 50%, a new peak started appearing at 17° with a significant
787 decrease in the intensity of the peak at 22°, suggesting a
788 mixture of poly(octylene adipate) and poly(octylene fur-
789 anoate) crystal phases. Upon further increase in DEFDC up to
790 75 and 90 mol %, the peak at 20° completely disappears. These
791 WAXS profiles of furan rich copolymers were very similar in
792 pattern to what was previously reported in the literature with
793 poly(octylene furanoate), suggesting that, at high furan
794 content, regardless of the presence of small amounts of diethyl
795 adipate, the crystalline structures of the copolymers are
796 dominated by the poly(octylene furanoate) crystal phase.³⁴
797 The pseudoeutectic behavior of these copolyesters is thus
798 confirmed by the WAXS results and is a characteristic of
799 isodimorphic copolymers showing an adipate-rich crystalline
800 phase at one side of the pseudoeutectic region, furan-rich
801 crystalline phase at the other, and the coexistence of both
802 crystalline phases at the pseudoeutectic point, which is
803 observed in the case of C_8 (50 mol %) in [Figure 5](#). This
804 does not mean that only one of the crystalline phases can exist
805 at either sides of the pseudoeutectic region but rather that the
806 two crystalline phases coexist at any given ratio of the two
807 repeating units; however, they appear as a single crystalline
808 phase resembling that of the repeating unit present in
809 abundance.^{21,64,69}

810 The influence of diol length was studied by comparing the
811 WAXS profiles of copolymers based on hexane-1,6-diol,
812 octane-1,8-diol, decane-1,10-diol, and dodecane-1,12-diol at a
813 constant 50 mol % DEFDC ratio as observed in [Figure S7](#). All
814 tested copolymers appeared to be semicrystalline in nature,
815 where C_6 (50 mol %) showed dominating peaks at 17° and 25°
816 belonging to furan-rich blocks, in addition to a minor peak at
817 14° that appeared to move gradually to lower θ angles as a
818 function of increasing the diol length, reaching 10° with C_{12}
819 (50 mol %), while maintaining a stable intensity. As the diol
820 length increased, peaks at 17° started to diminish and new
821 crystalline peaks at 21° belonging to the adipate-rich blocks
822 started appearing; where C_8 (50 mol %) showed a mixture of
823 both poly(octylene adipate) and poly(octylene furanoate)
824 crystal blocks, C_{10} (50 mol %) was dominated by poly-
825 (decylene adipate) crystals and small quantities of poly-

(decylene furanoate). However, with the longer dodecane- 826
1,12-diol, the peak belonging to poly(dodecylene furanoate) 827
disappeared, and the WAXS spectra was dominated with peaks 828
at 21° and 25°, suggesting the domination of the poly- 829
(dodecylene adipate) blocks. From these results, it appeared 830
that, at an equimolar DEFDC/diethyl adipate ratio, copoly- 831
mers based on longer diols had a stronger tendency to form 832
poly(alkylene adipate) rather than poly(alkylene furanoate) 833
crystals, as opposed to copolymers based on shorter diols that 834
had a quicker tendency to form the opposite. What was 835
generally observed in our work was that shorter diols reach the 836
pseudoeutectic transitional point at lower quantities of 837
DEFDC, whereas as evident in [Figure S7](#), at 50 mol % 838
DEFDC, polymers based on smaller diols such as hexane-1,6- 839
diol had already shifted toward furan-rich crystalline structures, 840
and octane-1,8-diol-based polymers appeared to be in very 841
close proximity to the pseudoeutectic point, while polymers 842
based on decane-1,10-diol and dodecane-1,12-diol maintained 843
adipate-rich crystalline structures even at 50% DEFDC. 844

845 CONCLUSION

846 The polycondensation reactions of different chain-length 846
aliphatic diols and diesters at a variable content of diethyl 847
furan-2,5-dicarboxylate (DEFDC) were studied using Novo- 848
zym 435 as biocatalyst. In agreement with previous reports in 849
the literature, an increase in the diol length was essential to 850
allow better reactivity toward DEFDC. However, the addition 851
of aliphatic diesters to synthesize terpolymers rather than 852
biopolymers was found to be better suited for CALB-mediated 853
catalysis, yielding polymers with M_n as high as 10 000 g·mol⁻¹ 854
even at elevated DEFDC content without the need for extreme 855
temperatures and long reaction times. On the other hand, the 856
reaction of dodecane-1,12-diol with different aliphatic diesters 857
in the presence of DEFDC showed no variations as a function 858
of DEFDC feed. Surprisingly though, copolymers produced in 859
the presence of long aliphatic diesters such as diethyl sebacate 860
had a low M_n when compared to reactions with diethyl oxalate 861
and diethyl adipate that had relatively similar results. The 862
introduction of the amorphous Pripol 2033 improved the 863
polymerization reaction in the systems containing high furan 864
content and butane-1,4-diol, which otherwise did not yield any 865
polymers without the long chain fatty dimer diol. The use of 866
such long fatty acid diols adjacent to the short chained diols 867
could be a promising approach, playing an important role in 868
future work to overcome some major limitations in enzymatic 869
catalysis toward the synthesis of semiaromatic polymers. Such 870
polymers can be used for food packaging, and this work has 871
introduced a green method to produce semiaromatic furan- 872
based copolyesters that could be further optimized, studied, 873
and compared with other semiaromatic copolyesters already on 874
the market such as polybutylene adipate terephthalate. 875

876 ASSOCIATED CONTENT

877 Supporting Information

878 The Supporting Information is available free of charge at 878
<https://pubs.acs.org/doi/10.1021/acsapm.1c01777>. 879

880 Additional ¹H and DOSY NMR spectra; additional 880
experiments; evolution of the composition of the 881
copolyesters vs reaction time; additional reaction 882
schemes; thermal properties of the copolyesters; 883
WAXS profiles of the copolyesters (PDF) 884

885 ■ AUTHOR INFORMATION

886 Corresponding Authors

887 **Philippe Zinck** – UMR 8181, UCCS, Unité de Catalyse et
888 Chimie du Solide, Univ. Lille, CNRS, Centrale Lille, Univ.
889 Artois, F-59000 Lille, France; orcid.org/0000-0003-2329-9116; Email: philippe.zinck@univ-lille.fr

891 **Jean-Marie Raquez** – Laboratory of Polymeric and Composite
892 Materials (LPCM), Center of Innovation and Research in
893 Materials and Polymers (CIRMAP), University of Mons,
894 7000 Mons, Belgium; orcid.org/0000-0003-1940-7129;
895 Email: jean-marie.raquez@umons.ac.be

896 Authors

897 **Kifah Nasr** – UMR 8181, UCCS, Unité de Catalyse et Chimie
898 du Solide, Univ. Lille, CNRS, Centrale Lille, Univ. Artois, F-
899 59000 Lille, France; Laboratory of Polymeric and Composite
900 Materials (LPCM), Center of Innovation and Research in
901 Materials and Polymers (CIRMAP), University of Mons,
902 7000 Mons, Belgium

903 **Audrey Favrelle-Huret** – UMR 8181, UCCS, Unité de
904 Catalyse et Chimie du Solide, Univ. Lille, CNRS, Centrale
905 Lille, Univ. Artois, F-59000 Lille, France; orcid.org/0000-0002-8510-9608

907 **Rosica Mincheva** – Laboratory of Polymeric and Composite
908 Materials (LPCM), Center of Innovation and Research in
909 Materials and Polymers (CIRMAP), University of Mons,
910 7000 Mons, Belgium

911 **Gregory Stoclet** – UMR 8207, UMET, Unité Matériaux et
912 Transformations, Univ. Lille, CNRS, INRAE, Centrale Lille,
913 59000 Lille, France; orcid.org/0000-0003-1510-0234

914 **Marc Brià** – Univ. Lille, CNRS, Centrale Lille, Univ. Artois,
915 FR 2638, IMEC–Plateforme RMN, Institut Michel-Eugène
916 Chevreul, F-59650 Villeneuve d'Ascq, France

917 Complete contact information is available at:

918 <https://pubs.acs.org/10.1021/acsapm.1c01777>

919 Author Contributions

920 Conceptualization: K.N., A.F.-H., J.-M.R., and P.Z.; method-
921 ology: K.N.; formal analysis: K.N.; WAXS analysis: G.S.;
922 DOSY analysis: M.B.; writing, original draft preparation: K.N.;
923 writing, review and editing: K.N., A.F.-H., J.-M.R., and P.Z.;
924 supervision: A.F.-H., J.-M.R., and P.Z.; project administration:
925 J.-M.R. and P.Z.; funding acquisition: J.-M.R. and P.Z. All
926 authors have read and agreed to the published version of the
927 manuscript.

928 Notes

929 The authors declare no competing financial interest.

930 ■ ACKNOWLEDGMENTS

931 This work was funded by the FWV ALPO Interreg Grant, and
932 the authors thank the European Regional Development Fund
933 (FEDER) and the University of Lille. Chevreul Institute (FR
934 2638), Ministère de l'Enseignement Supérieur, de la Recherche
935 et de l'Innovation, and Région Hauts de France are also
936 acknowledged for supporting and partially funding this work.
937 J.-M.R. is a FNRS research fellow at University of Mons. The
938 authors gratefully acknowledge Sébastien MOINS for the GPC
939 measurements.

■ REFERENCES

- (1) Babu, R. P.; O'Connor, K.; Seeram, R. Current Progress on Bio- 941
Based Polymers and Their Future Trends. *Prog. Biomater* **2013**, *2* (1), 942
8. 943
- (2) Aeschelmann, F.; Carus, M. Biobased Building Blocks and 944
Polymers in the World: Capacities, Production, and Applications— 945
Status Quo and Trends Towards 2020. *Industrial Biotechnology* **2015**, 946
11 (3), 154–159. 947
- (3) Caillol, S. Lifecycle Assessment and Green Chemistry: A Look at 948
Innovative Tools for Sustainable Development. In *Environmental* 949
Impact of Polymers; John Wiley & Sons, Ltd., 2014; pp 65–89; 950
DOI: 10.1002/9781118827116.ch5. 951
- (4) Hottle, T. A.; Bilec, M. M.; Landis, A. E. Sustainability 952
Assessments of Bio-Based Polymers. *Polym. Degrad. Stab.* **2013**, *98* 953
(9), 1898–1907. 954
- (5) Vilela, C.; Sousa, A. F.; Fonseca, A. C.; Serra, A. C.; Coelho, J. F. 955
J.; Freire, C. S. R.; Silvestre, A. J. D. The Quest for Sustainable 956
Polyesters – Insights into the Future. *Polym. Chem.* **2014**, *5* (9), 957
3119–3141. 958
- (6) van Putten, R.-J.; van der Waal, J. C.; de Jong, E.; Rasrendra, C. 959
B.; Heeres, H. J.; de Vries, J. G. Hydroxymethylfurfural, A Versatile 960
Platform Chemical Made from Renewable Resources. *Chem. Rev.* 961
2013, *113* (3), 1499–1597. 962
- (7) Kröger, M.; Prüße, U.; Vorlop, K.-D. A New Approach for the 963
Production of 2,5-Furandicarboxylic Acid by in Situ Oxidation of 5- 964
Hydroxymethylfurfural Starting from Fructose. *Top. Catal.* **2000**, *13* 965
(3), 237–242. 966
- (8) Koopman, F.; Wierckx, N.; de Winde, J. H.; Ruijsenaars, H. J. 967
Efficient Whole-Cell Biotransformation of 5-(Hydroxymethyl)- 968
Furfural into FDCA, 2,5-Furandicarboxylic Acid. *Bioresour. Technol.* 969
2010, *101* (16), 6291–6296. 970
- (9) Huang, Y.-T.; Wong, J.-J.; Huang, C.-J.; Li, C.-L.; Jang, G.-W. B. 971
2,5-Furandicarboxylic Acid Synthesis and Use. In *Chemicals and Fuels* 972
from Bio-Based Building Blocks; John Wiley & Sons, Ltd., 2016; pp 973
191–216; DOI: 10.1002/9783527698202.ch8. 974
- (10) Sousa, A. F.; Vilela, C.; Fonseca, A. C.; Matos, M.; Freire, C. S. 975
R.; Gruter, G.-J. M.; Coelho, J. F. J.; Silvestre, A. J. D. Biobased 976
Polyesters and Other Polymers from 2,5-Furandicarboxylic Acid: A 977
Tribute to Furan Excellency. *Polym. Chem.* **2015**, *6* (33), 5961–5983. 978
- (11) Dutta, S.; De, S.; Saha, B. A Brief Summary of the Synthesis of 979
Polyester Building-Block Chemicals and Biofuels from 5-Hydrox- 980
ymethylfurfural. *ChemPlusChem.* **2012**, *77* (4), 259–272. 981
- (12) Qian, X. Mechanisms and Energetics for Brønsted Acid- 982
Catalyzed Glucose Condensation, Dehydration and Isomerization 983
Reactions. *Top. Catal.* **2012**, *55* (3), 218–226. 984
- (13) Román-Leshkov, Y.; Chheda, J. N.; Dumesic, J. A. Phase 985
Modifiers Promote Efficient Production of Hydroxymethylfurfural 986
from Fructose. *Science* **2006**, *312* (5782), 1933–1937. 987
- (14) Collias, D. I.; Harris, A. M.; Nagpal, V.; Cottrell, I. W.; 988
Schultheis, M. W. Biobased Terephthalic Acid Technologies: A 989
Literature Review. *Industrial Biotechnology* **2014**, *10* (2), 91–105. 990
- (15) Burgess, S. K.; Karvan, O.; Johnson, J. R.; Kriegel, R. M.; Koros, 991
W. J. Oxygen Sorption and Transport in Amorphous Poly(Ethylene 992
Furanoate). *Polymer* **2014**, *55* (18), 4748–4756. 993
- (16) Knoop, R. J. I.; Vogelzang, W.; van Haveren, J.; van Es, D. S. 994
High Molecular Weight Poly(Ethylene-2,5-Furanoate); Critical 995
Aspects in Synthesis and Mechanical Property Determination. *J.* 996
Polym. Sci., Part A: Polym. Chem. **2013**, *51* (19), 4191–4199. 997
- (17) Zhu, J.; Cai, J.; Xie, W.; Chen, P.-H.; Gazzano, M.; Scandola, 998
M.; Gross, R. A. Poly(Butylene 2,5-Furan Dicarboxylate), a Biobased 999
Alternative to PBT: Synthesis, Physical Properties, and Crystal 1000
Structure. *Macromolecules* **2013**, *46* (3), 796–804. 1001
- (18) Lalanne, L.; Nyanhongo, G. S.; Guebitz, G. M.; Pellis, A. 1002
Biotechnological Production and High Potential of Furan-Based 1003
Renewable Monomers and Polymers. *Biotechnology Advances* **2021**, 1004
48, 107707. 1005
- (19) Pellis, A.; Malinconico, M.; Guarneri, A.; Gardossi, L. 1006
Renewable Polymers and Plastics: Performance beyond the Green. 1007
New Biotechnology **2021**, *60*, 146–158. 1008

- (20) Burgess, S. K.; Leisen, J. E.; Kraftschik, B. E.; Mubarak, C. R.; Kriegel, R. M.; Koros, W. J. Chain Mobility, Thermal, and Mechanical Properties of Poly(Ethylene Furanoate) Compared to Poly(Ethylene Terephthalate). *Macromolecules* **2014**, *47* (4), 1383–1391.
- (21) Terzopoulou, Z.; Papadopoulos, L.; Zamboulis, A.; Papageorgiou, D. G.; Papageorgiou, G. Z.; Bikiaris, D. N. Tuning the Properties of Furandicarboxylic Acid-Based Polyesters with Copolymerization: A Review. *Polymers* **2020**, *12* (6), 1209.
- (22) Llevot, A.; Grau, E.; Carlotti, S.; Grelier, S.; Cramail, H. Renewable (Semi)Aromatic Polyesters from Symmetrical Vanillin-Based Dimers. *Polym. Chem.* **2015**, *6* (33), 6058–6066.
- (23) Larrañaga, A.; Lizundia, E. A Review on the Thermomechanical Properties and Biodegradation Behaviour of Polyesters. *Eur. Polym. J.* **2019**, *121*, 109296.
- (24) Silvianti, F.; Maniar, D.; Boetje, L.; Loos, K. Green Pathways for the Enzymatic Synthesis of Furan-Based Polyesters and Polyamides. In *Sustainability & Green Polymer Chemistry Vol. 2: Biocatalysis and Biobased Polymers*; ACS Symposium Series; American Chemical Society, 2020; Vol. 1373, pp 3–29; DOI: 10.1021/bk-2020-1373.ch001.
- (25) Gandini, A.; Silvestre, A. J. D.; Neto, C. P.; Sousa, A. F.; Gomes, M. The Furan Counterpart of Poly(Ethylene Terephthalate): An Alternative Material Based on Renewable Resources. *J. Polym. Sci., Part A: Polym. Chem.* **2009**, *47* (1), 295–298.
- (26) Gomes, M.; Gandini, A.; Silvestre, A. J. D.; Reis, B. Synthesis and Characterization of Poly(2,5-Furan Dicarboxylate)s Based on a Variety of Diols. *J. Polym. Sci., Part A: Polym. Chem.* **2011**, *49* (17), 3759–3768.
- (27) Jiang, M.; Liu, Q.; Zhang, Q.; Ye, C.; Zhou, G. A Series of Furan-Aromatic Polyesters Synthesized via Direct Esterification Method Based on Renewable Resources. *J. Polym. Sci., Part A: Polym. Chem.* **2012**, *50* (5), 1026–1036.
- (28) Vannini, M.; Marchese, P.; Celli, A.; Lorenzetti, C. Fully Biobased Poly(Propylene 2,5-Furandicarboxylate) for Packaging Applications: Excellent Barrier Properties as a Function of Crystallinity. *Green Chem.* **2015**, *17* (8), 4162–4166.
- (29) Wang, J.; Liu, X.; Zhang, Y.; Liu, F.; Zhu, J. Modification of Poly(Ethylene 2,5-Furandicarboxylate) with 1,4-Cyclohexanedimethylene: Influence of Composition on Mechanical and Barrier Properties. *Polymer* **2016**, *103*, 1–8.
- (30) Lepoittevin, B.; Roger, P. Poly(Ethylene Terephthalate). In *Handbook of Engineering and Specialty Thermoplastics*; John Wiley & Sons, Ltd., 2011; pp 97–126; DOI: 10.1002/9781118104729.ch4.
- (31) Jia, Z.; Wang, J.; Sun, L.; Liu, F.; Zhu, J.; Liu, X. Copolyesters Developed from Bio-Based 2,5-Furandicarboxylic Acid: Synthesis, Sequence Distribution, Mechanical, and Barrier Properties of Poly(Propylene-Co-1,4-Cyclohexanedimethylene 2,5-Furandicarboxylate)s. *J. Appl. Polym. Sci.* **2019**, *136* (13), 47291.
- (32) Wang, J.; Mahmud, S.; Zhang, X.; Zhu, J.; Shen, Z.; Liu, X. Biobased Amorphous Polyesters with High T_g: Trade-Off between Rigid and Flexible Cyclic Diols. *ACS Sustainable Chem. Eng.* **2019**, *7* (6), 6401–6411.
- (33) Wang, X.; Wang, Q.; Liu, S.; Wang, G. Biobased Copolyesters: Synthesis, Structure, Thermal and Mechanical Properties of Poly(Ethylene 2,5-Furandicarboxylate-Co-Ethylene 1,4-Cyclohexanedimethyl dicarboxylate). *Polym. Degrad. Stab.* **2018**, *154*, 96–102.
- (34) Jiang, Y.; Woortman, A. J. J.; Alberda van Ekenstein, G. O. R.; Loos, K. A Biocatalytic Approach towards Sustainable Furanic-Aliphatic Polyesters. *Polym. Chem.* **2015**, *6* (29), 5198–5211.
- (35) Gross, R. A.; Ganesh, M.; Lu, W. Enzyme-Catalysis Breathes New Life into Polyester Condensation Polymerizations. *Trends Biotechnol.* **2010**, *28* (8), 435–443.
- (36) Chaudhary, A. K.; Lopez, J.; Beckman, E. J.; Russell, A. J. Biocatalytic Solvent-Free Polymerization To Produce High Molecular Weight Polyesters. *Biotechnol. Prog.* **1997**, *13* (3), 318–325.
- (37) Jacquet, N.; Freyermouth, F.; Fenouillot, F.; Rousseau, A.; Pascault, J. P.; Fuertes, P.; Saint-Loup, R. Synthesis and Properties of Poly(Butylene Succinate): Efficiency of Different Transesterification Catalysts. *J. Polym. Sci., Part A: Polym. Chem.* **2011**, *49* (24), 5301–5312.
- (38) Adrio, J. L.; Demain, A. L. Microbial Enzymes: Tools for Biotechnological Processes. *Biomolecules* **2014**, *4* (1), 117–139.
- (39) Jiang, Y.; Loos, K. Enzymatic Synthesis of Biobased Polyesters and Polyamides. *Polymers* **2016**, *8* (7), 243.
- (40) Cruz-Izquierdo, A.; van den Broek, L. A.M.; Serra, J. L.; Llama, M. J.; Boeriu, C. G. Lipase-Catalyzed Synthesis of Oligoesters of 2,5-Furandicarboxylic Acid with Aliphatic Diols. *Pure Appl. Chem.* **2015**, *87* (1), 59–69.
- (41) Jiang, Y.; Woortman, A. J. J.; Alberda van Ekenstein, G. O. R.; Petrović, D. M.; Loos, K. Enzymatic Synthesis of Biobased Polyesters Using 2,5-Bis(Hydroxymethyl)Furan as the Building Block. *Biomacromolecules* **2014**, *15* (7), 2482–2493.
- (42) Skoczinski, P.; Espinoza Cangahuala, M. K.; Maniar, D.; Albach, R. W.; Bittner, N.; Loos, K. Biocatalytic Synthesis of Furan-Based Oligomer Diols with Enhanced End-Group Fidelity. *ACS Sustainable Chem. Eng.* **2020**, *8* (2), 1068–1086.
- (43) Baraldi, S.; Fantin, G.; Di Carmine, G.; Ragno, D.; Brandolese, A.; Massi, A.; Bortolini, O.; Marchetti, N.; Giovannini, P. P. Enzymatic Synthesis of Biobased Aliphatic-Aromatic Oligoesters Using 5,5'-Bis(Hydroxymethyl)Furoin as a Building Block. *RSC Adv.* **2019**, *9* (50), 29044–29050.
- (44) Pellis, A.; Comerford, J. W.; Weinberger, S.; Guebitz, G. M.; Clark, J. H.; Farmer, T. J. Enzymatic Synthesis of Lignin Derivable Pyridine Based Polyesters for the Substitution of Petroleum Derived Plastics. *Nat. Commun.* **2019**, *10* (1), 1762.
- (45) Pellis, A.; Weinberger, S.; Gigli, M.; Guebitz, G. M.; Farmer, T. J. Enzymatic Synthesis of Biobased Polyesters Utilizing Aromatic Diols as the Rigid Component. *Eur. Polym. J.* **2020**, *130*, 109680.
- (46) Mueller, R.-J. Biological Degradation of Synthetic Polyesters—Enzymes as Potential Catalysts for Polyester Recycling. *Process Biochemistry* **2006**, *41* (10), 2124–2128.
- (47) Müller, R.-J.; Kleeberg, I.; Deckwer, W.-D. Biodegradation of Polyesters Containing Aromatic Constituents. *J. Biotechnol.* **2001**, *86* (2), 87–95.
- (48) Jian, J.; Xiangbin, Z.; Xianbo, H. An Overview on Synthesis, Properties and Applications of Poly(Butylene-Adipate-Co-Terephthalate)—PBAT. *Advanced Industrial and Engineering Polymer Research* **2020**, *3* (1), 19–26.
- (49) Kijchavengkul, T.; Auras, R.; Rubino, M.; Selke, S.; Ngouajio, M.; Fernandez, R. T. Biodegradation and Hydrolysis Rate of Aliphatic Aromatic Polyester. *Polym. Degrad. Stab.* **2010**, *95* (12), 2641–2647.
- (50) Herrera, R.; Franco, L.; Rodríguez-Galán, A.; Puiggali, J. Characterization and Degradation Behavior of Poly(Butylene Adipate-Co-Terephthalate)s. *J. Polym. Sci., Part A: Polym. Chem.* **2002**, *40* (23), 4141–4157.
- (51) Wu, B.; Xu, Y.; Bu, Z.; Wu, L.; Li, B.-G.; Dubois, P. Biobased Poly(Butylene 2,5-Furandicarboxylate) and Poly(Butylene Adipate-Co-Butylene 2,5-Furandicarboxylate)s: From Synthesis Using Highly Purified 2,5-Furandicarboxylic Acid to Thermo-Mechanical Properties. *Polymer* **2014**, *55* (16), 3648–3655.
- (52) Matos, M.; Sousa, A. F.; Fonseca, A. C.; Freire, C. S. R.; Coelho, J. F. J.; Silvestre, A. J. D. A New Generation of Furanic Copolyesters with Enhanced Degradability: Poly(Ethylene 2,5-Furandicarboxylate)-Co-Poly(Lactic Acid) Copolyesters. *Macromol. Chem. Phys.* **2014**, *215* (22), 2175–2184.
- (53) Sousa, A. F.; Guigo, N.; Pozycka, M.; Delgado, M.; Soares, J.; Mendonça, P. V.; Coelho, J. F. J.; Sbirrazzuoli, N.; Silvestre, A. J. D. Tailored Design of Renewable Copolymers Based on Poly(1,4-Butylene 2,5-Furandicarboxylate) and Poly(Ethylene Glycol) with Refined Thermal Properties. *Polym. Chem.* **2018**, *9* (6), 722–731.
- (54) Wu, L.; Mincheva, R.; Xu, Y.; Raquez, J.-M.; Dubois, P. High Molecular Weight Poly(Butylene Succinate-Co-Butylene Furandicarboxylate) Copolyesters: From Catalyzed Polycondensation Reaction to Thermomechanical Properties. *Biomacromolecules* **2012**, *13* (9), 2973–2981.
- (55) Yu, Z.; Zhou, J.; Cao, F.; Wen, B.; Zhu, X.; Wei, P. Chemosynthesis and Characterization of Fully Biomass-Based

- 1146 Copolymers of Ethylene Glycol, 2,5-Furandicarboxylic Acid, and
1147 Succinic Acid. *J. Appl. Polym. Sci.* **2013**, *130* (2), 1415–1420.
- 1148 (56) Zhou, W.; Wang, X.; Yang, B.; Xu, Y.; Zhang, W.; Zhang, Y.; Ji,
1149 J. Synthesis, Physical Properties and Enzymatic Degradation of Bio-
1150 Based Poly(Butylene Adipate-Co-Butylene Furandicarboxylate) Co-
1151 polyesters. *Polym. Degrad. Stab.* **2013**, *98* (11), 2177–2183.
- 1152 (57) Morales-Huerta, J. C.; Ciulik, C. B.; de Ilarduya, A. M.; Munoz-
1153 Guerra, S. Fully Bio-Based Aromatic–Aliphatic Copolyesters: Poly-
1154 (Butylene Furandicarboxylate-Co-Succinate)s Obtained by Ring
1155 Opening Polymerization. *Polym. Chem.* **2017**, *8* (4), 748–760.
- 1156 (58) Maniar, D.; Jiang, Y.; Woortman, A. J. J.; van Dijken, J.; Loos,
1157 K. Furan-Based Copolyesters from Renewable Resources: Enzymatic
1158 Synthesis and Properties. *ChemSusChem* **2019**, *12* (5), 990–999.
- 1159 (59) Nasr, K.; Meimoun, J.; Favrelle-Huret, A.; Winter, J. D.;
1160 Raquez, J.-M.; Zinck, P. Enzymatic Polycondensation of 1,6-
1161 Hexanediol and Diethyl Adipate: A Statistical Approach Predicting
1162 the Key-Parameters in Solution and in Bulk. *Polymers* **2020**, *12* (9),
1163 1907.
- 1164 (60) Azim, H.; Dekhterman, A.; Jiang, Z.; Gross, R. A. Candida
1165 Antarctica Lipase B-Catalyzed Synthesis of Poly(Butylene Succinate):
1166 Shorter Chain Building Blocks Also Work. *Biomacromolecules* **2006**, *7*
1167 (11), 3093–3097.
- 1168 (61) Mahapatro, A.; Kalra, B.; Kumar, A.; Gross, R. A. Lipase-
1169 Catalyzed Polycondensations: Effect of Substrates and Solvent on
1170 Chain Formation, Dispersity, and End-Group Structure. *Biomacromo-
1171 lecules* **2003**, *4* (3), 544–551.
- 1172 (62) Debuissy, T.; Pollet, E.; Avérous, L. Enzymatic Synthesis of a
1173 Bio-Based Copolyester from Poly(butylene succinate) and Poly((R)-
1174 3-hydroxybutyrate): Study of Reaction Parameters on the Trans-
1175 esterification Rate. *Biomacromolecules* **2016**, *17* (12), 4054–4063.
- 1176 (63) Bazin, A.; Avérous, L.; Pollet, E. Lipase-Catalyzed Synthesis of
1177 Furan-Based Aliphatic-Aromatic Biobased Copolyesters: Impact of
1178 the Solvent. *Eur. Polym. J.* **2021**, *159*, 110717.
- 1179 (64) Pérez-Camargo, R. A.; Arandia, I.; Safari, M.; Cavallo, D.; Lotti,
1180 N.; Soccio, M.; Müller, A. J. Crystallization of Isodimorphic Aliphatic
1181 Random Copolyesters: Pseudo-Eutectic Behavior and Double-
1182 Crystalline Materials. *Eur. Polym. J.* **2018**, *101*, 233–247.
- 1183 (65) Mincheva, R.; Delangre, A.; Raquez, J.-M.; Narayan, R.;
1184 Dubois, P. Biobased Polyesters with Composition-Dependent
1185 Thermomechanical Properties: Synthesis and Characterization of
1186 Poly(Butylene Succinate-Co-Butylene Azelate). *Biomacromolecules*
1187 **2013**, *14* (3), 890–899.
- 1188 (66) Liang, Z.; Pan, P.; Zhu, B.; Inoue, Y. Isomorphic Crystallization
1189 of Aliphatic Copolyesters Derived from 1,6-Hexanediol: Effect of the
1190 Chemical Structure of Comonomer Units on the Extent of
1191 Cocrystallization. *Polymer* **2011**, *52* (12), 2667–2676.
- 1192 (67) Kwiatkowska, M.; Kowalczyk, I.; Kwiatkowski, K.; Szymczyk,
1193 A.; Jędrzejewski, R. Synthesis and Structure – Property Relationship
1194 of Biobased Poly(Butylene 2,5-Furanoate) – Block – (Dimerized
1195 Fatty Acid) Copolymers. *Polymer* **2017**, *130*, 26–38.
- 1196 (68) Bai, Z.; Liu, Y.; Su, T.; Wang, Z. Effect of Hydroxyl Monomers
1197 on the Enzymatic Degradation of Poly(Ethylene Succinate), Poly-
1198 (Butylene Succinate), and Poly(Hexylene Succinate). *Polymers* **2018**,
1199 *10* (1), 90.
- 1200 (69) Ceccorulli, G.; Scandola, M.; Kumar, A.; Kalra, B.; Gross, R. A.
1201 Cocrystallization of Random Copolymers of ω -Pentadecalactone and
1202 ϵ -Caprolactone Synthesized by Lipase Catalysis. *Biomacromolecules*
1203 **2005**, *6* (2), 902–907.